Geophys. J. Int. (2005) **162,** 332–336 doi: 10.1111/j.1365-246X.2005.02671.x

Comment on 'Electrical conductivity and crustal structure beneath the central Hellenides around the Gulf of Corinth (Greece) and their relationship with the seismotectonics' by Pham *et al.*

I. I. Rokityansky,[1] P. Varotsos[2,3] and N. Sarlis[3]

[1]*Institute of Geophysics, National Academy of Sciences of Ukraine, POB-70, Kiev-146, Ukraine. E-mail: irokityansky@yahoo.com*
[2]*Solid Earth Physics Institute, University of Athens, Panepistimiopolis, Zografos 157 84, Athens, Greece. E-mail: pvaro@otenet.gr*
[3]*Solid State Section, Department of Physics, University of Athens, Panepistimiopolis, Zografos 157 84, Athens, Greece E-mail: nsarlis@cc.uoa.gr*

Accepted 2005 April 1. Received 2005 January 15; in original form 2003 July 18

SUMMARY

This comment discusses the analysis of magnetotelluric data from the Corinth Gulf area carried out by Pham *et al.* It is shown that a consistent analysis should include the conducting sea water of the Gulf, which has a longitudinal conductance of about 2000 S. This was overlooked in the above study. The magnitude of the sea-water effect is demonstrated by 2-D modelling and new induction vector data.

Key words: crustal structure, electrical anisotropy, Gulf of Corinth, magnetotellurics.

1 INTRODUCTION

A magnetotelluric (MT) study of the western part of the Gulf of Corinth was described by Pham *et al*. (2000). They reported a complex geoelectric crustal structure, and the most prominent feature of their model was a relatively conductive layer, 4-km thick, at a depth greater than 10 km. Pham *et al.* (2000) also concluded that the geotectonic structure of the Parnassos unit and the Transition zone in the central Hellenides is clearly identified by its higher resistivity, and that its intrinsic anisotropy is related to the north–south strike of the Hellenides range.

If true, these results are important for several reasons. They are, for example, related to the debate regarding the possible transmission of Seismic Electric Signals (SES) (e.g. Varotsos & Lazaridou 1991; Uyeda *et al.* 2000, 2002). SES are only observed in certain places, and this selectivity can be explained by heterogeneities in the Earth's crust (Varotsos & Alexopoulos 1986; Varotsos *et al.* 1993). This idea is supported by both numerical simulations (Sarlis *et al.* 1999) and analytical solutions (Varotsos *et al.* 2000). The purpose of this comment is to clarify what conclusions can be made about the geoelectric structure around the Gulf of Corinth, based on the data of Pham *et al.* (2000).

2 DESCRIPTION OF THE MAGNETOTELLURIC DATA

Fig. 1 shows the locations at which MT data were collected by Pham *et al.* (2000), and Fig. 2 presents the data as maps of the apparent resistivity. At short periods ($T = 1/200$ s) both polarizations of the MT impedance data show a three-dimensional (3-D) shallow geoelectric structure, with quite high values of apparent resistivity (1000 Ωm) in the centre of the study area and low values near Sataina and the Gulf of Corinth. At longer periods ($T = 50$ s) the 3-D behaviour is again obvious, but, in the central part of the area, low apparent resistivities are observed. Pham *et al.* (2000) interpreted this as a conductive layer at a depth of 10 km. However, it could also be explained for the E-polarization by the inductive influence of the sea-water conductor (400-m deep Corinth Gulf) located at approximately the same distance (10 km) from MT stations in the middle of the array shown in Fig. 1. Pham *et al.* (2000) presented the observed MT data in the form of pseudo-sections of apparent resistivity for NS and EW directions along the four profiles in Fig. 1, but did not show the phase data. The E-polarization and B-polarization apparent resistivity pseudo-sections are quite different, probably as a result of the static shift effect.

3 EFFECT OF THE GULF OF CORINTH ON ONSHORE MT DATA

To investigate the effect of the low-resistivity sea water, a modelling exercise was undertaken. Using bathymetry data of the Corinth Gulf along profiles against the Psaromita and Pangalos peninsulas and against Patras, with azimuths of 20°, 10° and –30° respectively, three 2-D models of the Corinth Gulf were constructed. The results of the modelling for the first profile, coincident with the profile AA′ BB′ in Fig. 1, are presented in Fig. 3. The resistivity of the half-space was intentionally selected to be very low, i.e. 100 Ωm, in order to obtain a minimum estimate of the effect of the sea water. Nevertheless, near the Gulf coast the divergence of the E- and B-polarization apparent resistivity curves exceeds two orders of magnitude. This difference becomes one order of magnitude at a distance of 2 km from the coast for the period 10 s. Several models were constructed with more realistic cross-sections, using (a) a half-space with a resistivity of 200, 400, 500 and 1000 Ωm, (b) an upper layer 1-km thick

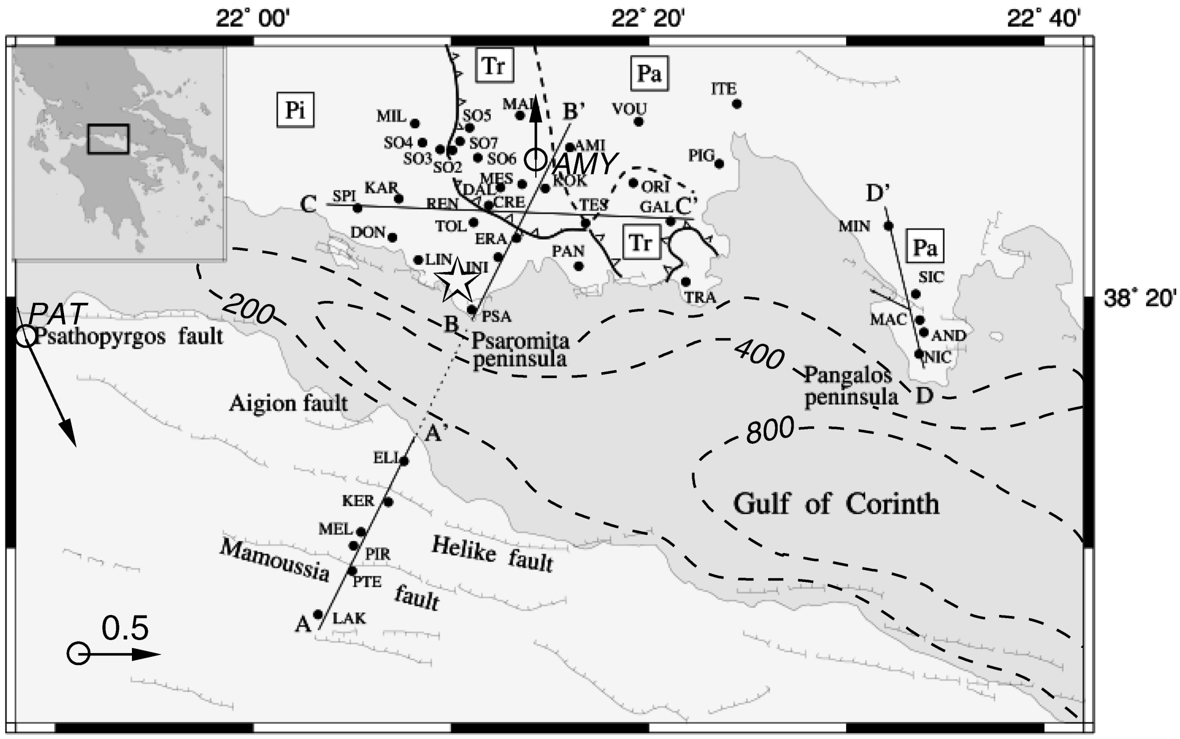

Figure 1. Location of the MTS stations in the Corinth Gulf area. Heavy solid curve with triangles: overthrust; dashed curve: upthrust, which separates the Pindos (Pi), the Transition (Tr) and the Parnassos (Pa) tectonic zones. The straight lines indicate the profiles interpreted in Pham *et al.* (2000). The star shows the epicentre of the Aigio-Eratini earthquake (magnitude $M_s = 6.2$) that occurred on 1995 June 15. The open circles are the locations of new induction vector measurements: the arrow depicts the real induction vector for the period 100 s.

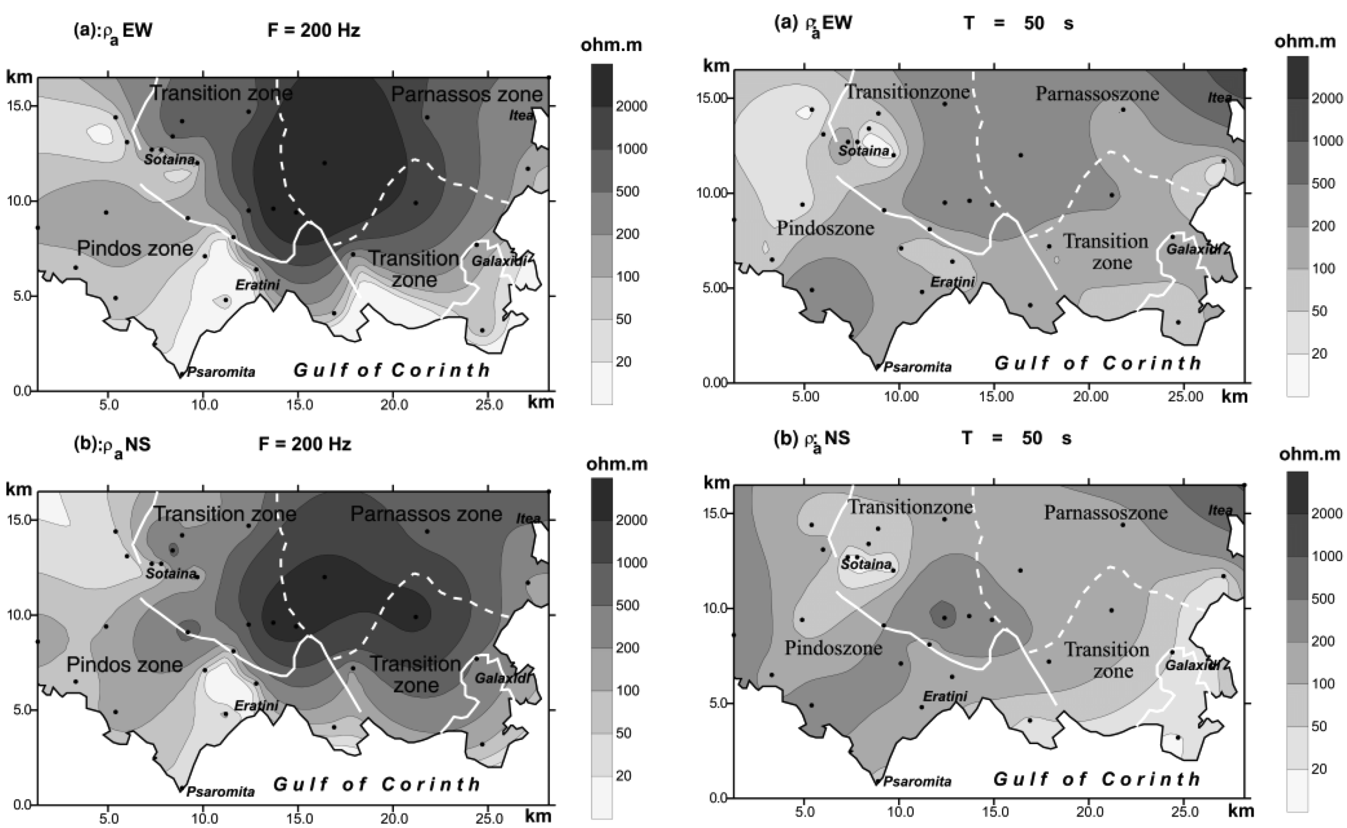

Figure 2. Apparent resistivity maps on the northern side of the Corinth Gulf for frequencies of 200 and 0.02 Hz for two principal directions. ρ_{EW} – upper panels; ρ_{NS} – lower panels from Pham *et al.* (2000).

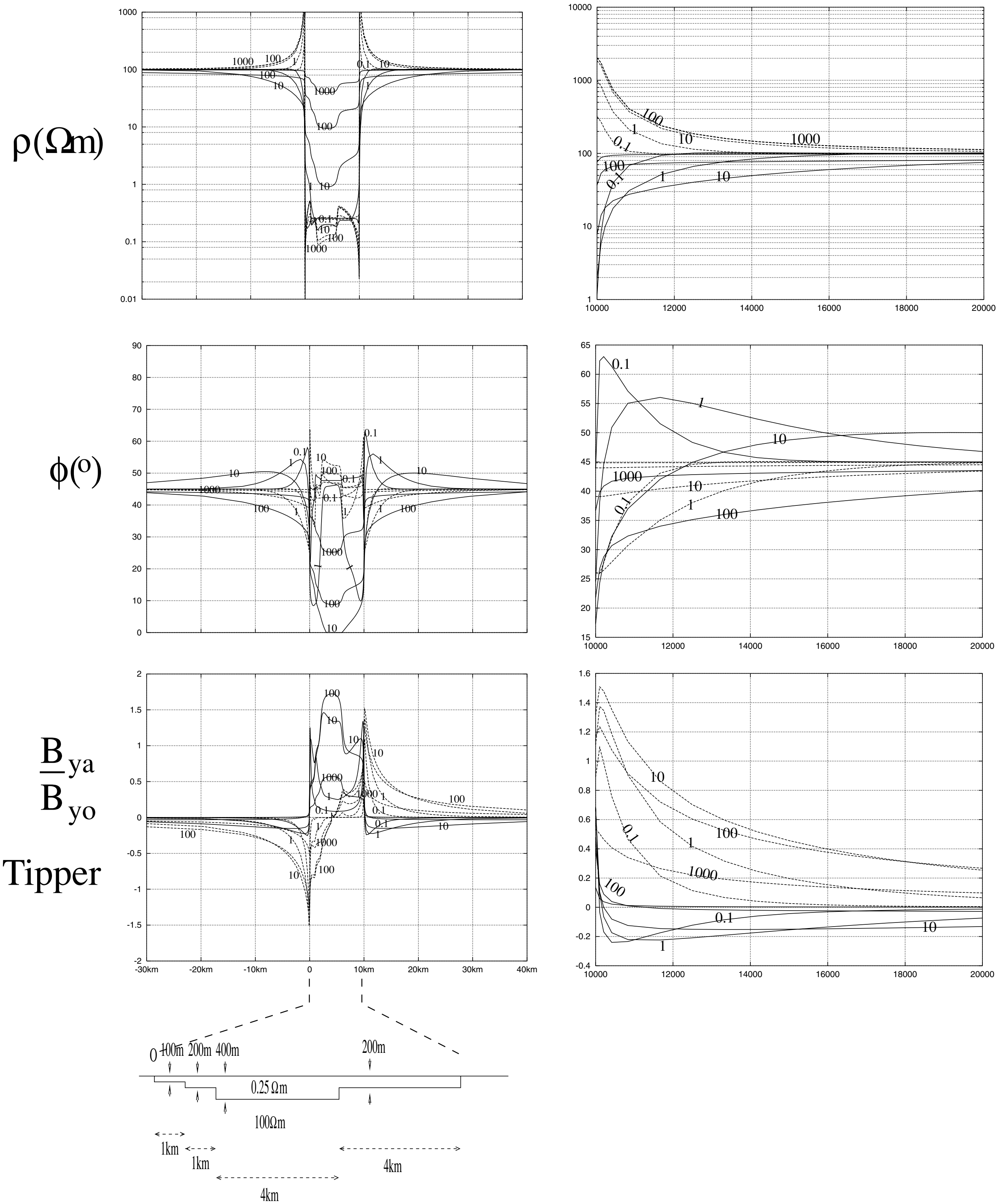

Figure 3. Results of our 2-D modelling of the Corinth Gulf sea water (resistivity 0.25 Ωm) embedded in a half-space with resistivity 100 Ωm along the profile AA′–BB′. Profile curves of MTS parameters ρ and phase ϕ are depicted by solid lines for E-polarization, and by dotted lines for B-polarization. MVP profile curves: for the horizontal field they are given by solid lines, while for the vertical field (tipper) they are given by dotted lines. In the two columns the same results are presented with different spatial scales: on the right, an enlarged version is given for the northern part of the profile. The cross-section of the model is shown at the bottom. The index of the curves gives the period in seconds.

with a resistivity of 100 Ωm underlain by a more resistive (500 and 2000 Ωm) lithosphere 100-km thick and deep varying with depth upper mantle conductivity structure as the optimal model in Eftaxias *et al.* (2002), and (e) the same as (b) but with the crustal layer at a depth of 10–14 km and with a resistivity of 70 Ωm. All these diverse models show that in land sites the sea water lowers the apparent resistivity of E-polarization and raises the apparent resistivity of the B-polarization, and creates a regional anisotropy of the MT field. The modelling shows a difference of apparent resistivity for the two polarizations ranging from a factor of 2 to three orders of magnitude for periods 1–100 s, depending on the distance from the sea water (for the strip 10 km wide) and the parameters used for the underlying layered structure. Such regional anisotropy should be easily detected and it is surprising that it was not reported by Pham *et al.* (2000).

Induction vectors were obtained for Amygdalea, 10 km north of the Gulf of Corinth, in a joint study by the Solid Earth Physics Institute of Athens University and the Institute of Geophysics of the Polish Academy of Sciences (under Prof. R. Teisseyre and Dr T. Ernst) and for Patras, 30 km west from the MTS array of Pham *et al.* (2000), near the southern coast of the Gulf (Figs 1 and 4).

For Amygdalea, at all periods the real (in-phase) induction vector points steadily north, thus indicating that the anomalous conductor is located to the south of the observation site and has EW strike. The magnitude of the vector steadily increases with decreasing period for the interval 700–100 s and attains a value of 0.45 at $T = 100$ s. At the same time, the imaginary (out-of-phase) vector points exactly south. Such anti-parallelism of real and imaginary vectors indicates: (1) 2-D behaviour of anomalous sea currents; and (2) that the maximum of the frequency characteristics of the anomalous geomagnetic variation field lies at a period T_{O} shorter than 100 s (see Rokityansky 1982, pp. 286–288). The results of the 2-D modelling presented in Fig. 3 yield the following behaviour: the real induction vector (tipper) attains a maximal magnitude of 0.3 at $T_{\mathrm{O}} = 40$ s and rapidly diminishes at long periods. To fit the observed vector magnitude of 0.45 at $T = 100$ s we present in Fig. 4 (right lower graph) results for the Corinth Gulf model with a resistivity of the embedding half-space of 400 Ωm. For periods of 100 and 160 s we see good agreement, but at longer periods the calculated Cu run well below the observed data, shown with open circles. From our previous study (Eftaxias *et al.* 2002) we know that at long periods of 300–6000 s the effect of the deep (1000–3000 m) sea water of the Ionian, Mediterranean and the southern Aegean seas persists in the formation of induction vectors in Greece. The distance to the deep water of the seas exceeds 150 km, so the correct choice of normal cross-section is of primary importance. Eftaxias *et al.* (2002) calculated the Ionian sea effect for more than 50 versions of normal cross-section, and found that the models containing an asthenosphere with conductance 1000–2000 S at a depth of 100 km yield the best fit with observations in the Ioannina area. The curves labelled as 'Ion' in Fig. 4 are the results of our previous study.

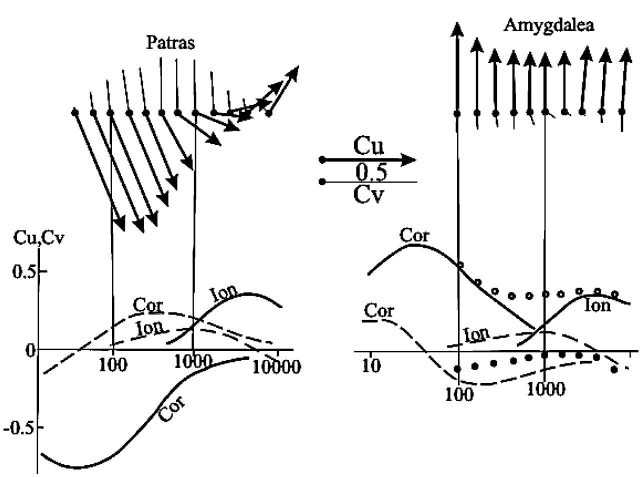

Figure 4. Induction vectors observed in Patras (for periods 40–6000 s) and Amygdalea (for periods 100–6000 s). The real vectors **Cu** are given in Wiese convention ('from conductor') by solid arrows, and the imaginary (out-of-phase or quadrature) ones **Cv** are given by thin solid lines. In the lower graphs, the results of 2-D modelling of the sea-water effect are presented: Cu by solid lines, Cv by dashed lines. Curves labelled 'Cor' present the effect of the Corinth Gulf, and those labelled by 'Ion' the effect of the Ionian, Mediterranean and southern part of the Aegean seas. Open and solid circles in Amygdalea present observed data for Cu and Cv, respectively.

The Corinth Gulf and deep seas are well separated spatially (>150 km) and temporally (in the frequency domain $T_{\mathrm{O}} = 40$ and 4000 s), so we can neglect the mutual influence of the anomalous currents in the Corinth Gulf and deep seas and consider induction vectors from the two objects as additive ones. Fig. 4 supports this suggestion. For the Amygdalea site the induction vectors are parallel at all periods, meaning that the effective resulting anomalous currents both in the Gulf and in the deep seas are approximately parallel, which allows algebraic superposition, as in the right bottom graphs of Fig. 4. It can be seen that the superposition of calculated tippers from the Gulf ('Cor') and deep seas ('Ioa') coincide very closely with the observed data for both real and imaginary vectors.

In Patras, the real vector at periods of 40–250 s points SSE (azimuth 157°, i.e. normal to the local Corinth Gulf strike) and attains a magnitude of 0.77, while the imaginary vector decreases to zero at a period of 40 s. The integrated effect of the deep seas gives an induction vector at the longest period of 6300 s with an azimuth of 25°. The reason for this is clear: Patras is located approximately 50 km nearer than Amygdalea to the Ionian Sea with a deep water strike in a NW–SE direction. It is clear that the superposition of induction vectors from the Gulf and deep seas should be done geometrically. Doing this with the calculated tippers ('Cor' has azimuth 157° and 'Ion' has azimuth 25°) given in the lower left graphs of Fig. 4, one can obtain real and imaginary induction vectors that are in good agreement with the observed data (Fig. 4 upper right).

4 DISCUSSION AND CONCLUSIONS

The modelling and data collection described above have shown that the Gulf of Corinth has a dominant effect on MT and induction vector data in the period range 3–300 s. This effect was not noted and taken into account in the study of Pham *et al.* (2000). Thus, the main result of Pham *et al.* (2000) on the existence of a crustal high-conductivity layer at a depth of 10–14 km is questionable. To gain an understanding of the deep conductivity structure beneath the central Hellenides around the Gulf of Corinth the following steps should be undertaken.

(1) A thorough impedance tensor analysis to define dimensionality and principal directions and to separate regional and local conductivity influences.

(2) Modelling of the sea-water effects with different versions of land conductivity and normal deep conductivity cross-sections in both 2-D and thin-film quasi-3-D approaches.

(3) Comparison of the results of the above two points, i.e. observed and modelled fields (their spatial and frequency

dependences) in order to form a conclusion (or suggestion) on the deep conductivity structure.

(4) Checking of the conclusion (suggestion) by adequate 3-D or 2-D modelling.

If the impedance tensor behaviour turns out to be regionally 2-D (although the data of Fig. 2 do not support such a suggestion), the last three points can be replaced by 2-D inversion.

ACKNOWLEDGMENTS

We express our sincere thanks to Professor R. Teisseyre and Dr T. Ernst (Institute of Geophysics of the Polish Academy of Science), who participated in the field measurements of the MT field to the north of Corinth Gulf and kindly allowed us to present some MVP data here.

REFERENCES

Eftaxias, K., Rokityansky, I.I., Bogris, N., Balasis, G. & Varotsos, P., 2002. Magnetovariational and magnetotelluric study of Ioannina region sensitive to Seismic Electric Signals (SES), *J. Atm. Electricity*, **22**, 113–137.

Pham, V.N., Bernard, P., Boyer, D., Chouliaras, G., Le Mouël, J.L. & Stavrakakis, G.N., 2000. Electrical conductivity and crustal structure beneath the central Hellenides around the Gulf of Corinth (Greece) and their relationship with the seismotectonics, *Geophys. J. Int.*, **142**, 948–969.

Rokityansky, I.I., 1982. *Geoelectromagnetic Investigation of the Earth's Crust and Mantle*, Springer-Verlag, Berlin, 381pp.

Sarlis, N., Lazaridou, M., Kapiris, P. & Varotsos, P., 1999. Numerical model of the selectivity effect and the $\Delta V/L$ criterion, *Geophys. Res. Lett.*, **26**, 3245–3248.

Uyeda, S., Nagao, T., Orihara, Y., Yamaguchi, T. & Takahashi, I., 2000. Geoelectric potential changes: Possible precursors to earthquakes in Japan, *Proc. Nat. Acad. Sci*, **97**, 4561–4566.

Uyeda, S. *et al.*, 2002. Electric and magnetic phenomena observed before the volcano-seismic activity in 2000 in the Izu Island Region, Japan, *Proc. Natl Acad. Sci. USA*, **99**, 7352–7355.

Varotsos, P. & Alexopoulos, K., 1986. *Thermodynamics of Point Defects and their Relation with Bulk Properties*, North Holland, Amsterdam.

Varotsos, P. & Lazaridou, M., 1991. Latest aspects of earthquake prediction in Greece based on Seismic Electric Signals, *Tectonophysics*, **188**, 321–347.

Varotsos, P., Alexopoulos, K. & Lazaridou, M., 1993. Latest aspects of earthquake prediction in Greece based on seismic electric signals, II, *Tectonophysics*, **224**, 1–37.

Varotsos, P., Sarlis, N. & Lazaridou, M., 2000. Transmission of stress induced electric signals in dielectric media, Part II, *Acta Geophys. Pol.*, **48**, 141–177.